



NIST Special Publication 260
NIST SP 260-243

Certification of
Standard Reference Material® 1595a
Tripalmitin

Michael A. Nelson
Jerome Mulloor
Brian E. Lang
Blaza Toman
Antonio Possolo
William J. Perry
Alicia N. Lyle

This publication is available free of charge from:
<https://doi.org/10.6028/NIST.SP.260-243>

Page Intentionally Blank

NIST Special Publication 260
NIST SP 260-243

Certification of Standard Reference Material® 1595a Tripalmitin

Michael A. Nelson, Jerome Mulloor, Brian E. Lang
*Chemical Sciences Division
Material Measurement Laboratory
National Institute of Standards and Technology*

Blaza Toman, Antonio Possolo
*Statistical Engineering Division
Information Technology Laboratory
National Institute of Standards and Technology*

William J. Perry, Alicia N. Lyle
*Division of Laboratory Sciences
National Center for Environmental Health
U.S. Centers for Disease Control and Prevention*

This publication is available free of charge from:
<https://doi.org/10.6028/NIST.SP.260-243>

March 2024



U.S. Department of Commerce
Gina M. Raimondo, Secretary

National Institute of Standards and Technology
Laurie E. Locascio, NIST Director and Under Secretary of Commerce for Standards and Technology

NIST SP 260-243
March 2024

Certain commercial entities, equipment, or materials may be identified in this document in order to describe an experimental procedure or concept adequately. Such identification is not intended to imply recommendation or endorsement by the National Institute of Standards and Technology, nor is it intended to imply that the entities, materials, or equipment are necessarily the best available for the purpose.

NIST Technical Series Policies

[Copyright, Fair Use, and Licensing Statements](#)

[NIST Technical Series Publication Identifier Syntax](#)

Publication History

Approved by the NIST Editorial Review Board on 2024-01-29

How to Cite this NIST Technical Series Publication

Nelson MA, Mulloor J, Lang BE, Toman B, Possolo A, Perry WJ, Lyle AN (2024) Certification of Standard Reference Material® 1595a Tripalmitin. (National Institute of Standards and Technology, Gaithersburg, MD), NIST Special Publication (SP) NIST SP 260-243. <https://doi.org/10.6028/NIST.SP.260-243>.

NIST Author ORCID iDs

Nelson MA: 0000-0003-0503-4501
Mulloor J: 0000-0002-7516-2165
Lang BE: 0000-0002-0772-1420
Toman B: 0000-0002-0999-9565
Possolo A: 0000-0002-8691-4190
Perry WJ: 0000-0002-0570-6956
Lyle AN: 0000-0001-7527-9200

Contact Information

Please address technical questions you may have about this SRM to srms@nist.gov where they will be assigned to the appropriate Technical Project Leader responsible for support of this material. For sales and customer service inquiries, please contact srminfo@nist.gov

Abstract

Standard Reference Material (SRM) 1595a Tripalmitin is a high purity chemical substance having a certified value for purity, expressed as a mass fraction. It is intended for use in preparing calibrants for measurement of total glycerides in clinical samples. A unit of SRM 1595a consists of one bottle containing 2 g of tripalmitin powder. This publication documents the production, analytical methods, and computations involved in characterizing this product.

Keywords

Markov Chain Monte Carlo (MCMC); purity determination; quantitative proton nuclear magnetic resonance spectroscopy with internal standard (^1H -qNMR); Standard Reference Material (SRM); thermal gravimetric analysis (TGA); triglyceride measurement procedure standard; tripalmitin.

Table of Contents

1. Introduction	1
2. Production	3
3. Material Suitability Assessment	4
3.1. Materials	4
3.2. Sample Preparation	4
3.3. Instrumentation and Signal Analysis	4
3.4. Identification	5
3.4.1. NMR Spectroscopy	5
3.4.2. High Resolution Mass Spectral Evaluation	8
3.5. Quantitative Analysis	8
3.5.1. Experimental Design	9
3.5.2. Spectral Integral Selection	10
3.5.3. Sample Purity Estimates	11
3.5.4. Influence of Run, Jar, Sample, and Software Factors	12
3.5.5. Influence of ¹ H-NMR Analysis Order	15
3.5.6. Estimated Purity	15
3.5.7. Conclusions	17
4. ¹H-NMR Purity and Homogeneity Assessment	18
4.1. Materials	18
4.2. Sample Preparation	18
4.3. Analysis	19
4.3.1. ¹ H-qNMR _{IS} Evaluation	19
4.3.2. ¹ H-qNMR _{IS} Purity	22
5. Water	28
5.1. Materials	28
5.2. Karl Fischer Titration	28
5.3. Thermogravimetric Analysis	30
5.4. Summary	32
References	33
Appendix A. List of Abbreviations and Acronyms	35

List of Tables

Table 1. Summary of ¹H-NMR Spectrum Peaks Evaluated for qNMR Purity Analysis.	6
Table 2. Measured Parameter Values for Jar 1 and Jar 2 Samples.	12
Table 3. Tripalmitin Purity Determined Using Integrals of the 2.3 ppm Spectral Interval.....	12
Table 4. Two-Way ANOVA Assessment of Between-Run and Between-Replicate Variance.	13
Table 5. Two-Way ANOVA Assessment of Between-Jar and Between-Replicate Variance.....	13
Table 6. One-Way ANOVA Assessment of Between-Sample Variance.	14
Table 7. One-Way ANOVA Assessment of Between-Software Variance.	14
Table 8. One-Way ANOVA Assessment of Between-Software Variance.	16
Table 9. Sampling Scheme	18
Table 10. Sample-Specific Measurement inputs and Purity Estimates.	21
Table 11. Maximum Likelihood Beta Parameters and Their Covariance Matrix.....	26
Table 12. Karl Fischer Water Measurement Summary.	30
Table 13. Thermal Gravimetric Analysis Water Measurement Summary.	31

List of Figures

Fig. 1. Chemical Structure of Tripalmitin.	1
Fig. 2. Sales History of SRM 1595.	1
Fig. 3. Location of Customers for SRM 1595 Tripalmitin.	2
Fig. 4. Chemical Structure of Tecnazene.	4
Fig. 5. Exemplary ¹H Spectrum of Bulk Candidate SRM 1595a Tripalmitin in CDCl₃.	6
Fig. 6. Comparison of ¹H Spectral Regions for SRM 1595 and SRM 1595a.	7
Fig. 7. ¹H-¹³C HSQC Spectrum of Bulk Candidate SRM 1595a Tripalmitin in CDCl₃ with ¹H-¹³C Correlation Assignments.	7
Fig. 8. ¹H-¹³C HMBC Spectrum of Bulk Candidate SRM 1595a Tripalmitin in CDCl₃.	8
Fig. 9. Experimental Design for the Analysis of Bulk Candidate SRM 1595a Tripalmitin Purity.	9
Fig. 10. Purity Values Calculated Using Integrals for Three ¹H Spectral Regions.	10
Fig. 11. Purity Value Distributions for Integrals From Three ¹H Spectral Regions.	11
Fig. 12. Boxplots of Purity Values Comparing Run, Jar, and Software Factors.	14
Fig. 13. Measured Purity Values and Standard Deviation as Functions of Analysis Order.	15
Fig. 14. Comparison of the Candidate SRM 1595a Tripalmitin ¹H Spectra Before and After Bottling. ...	19
Fig. 15. Integration Regions Used to Calculate Peak Areas.	20
Fig. 16. Sample-Specific Purities as Functions of ¹H-NMR Analysis and Bottle Fill Orders.	22
Fig. 17. Comparison of Purity Distributions for Units Derived from Jar 1 and Jar 2 Materials.	24
Fig. 18. SRM 1595a Purity Distributions.	25
Fig. 19. Beta Distribution Approximation to the MCMC Posterior Distribution.	26
Fig. 20. Sample-Specific Water Content as Functions of TGA Analysis and Bottle Fill Orders.	32

Acknowledgments

We thank Uliana Danilenko and Hubert W. Vesper of the U.S. Centers for Disease Control and Prevention, National Center for Environmental Health, Division of Laboratory Services (CDC-NCEH-DLS) for their assistance with high resolution mass spectrometric evaluations of the bulk tripalmitin materials used to produce SRM 1595a.

1. Introduction

Tripalmitin is a triglyceride obtained by formal acylation of the three hydroxy groups of glycerol by palmitic (hexadecanoic) acid. The chemical structure of tripalmitin is displayed in Fig. 1; tripalmitin is achiral.

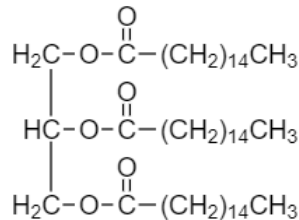


Fig. 1. Chemical Structure of Tripalmitin.

SRM 1595a is the successor to SRM 1595 Tripalmitin [1], which was used in the calibration and standardization of procedures for the chemical analysis of serum for triglycerides and for the critical evaluation of routine working or secondary reference materials used in these procedures. Notably, SRM 1595 was used in the preparation of calibration standards for the total glycerides Reference Measurement Procedure (RMP) [2] maintained by the Centers for Disease Control and Prevention, National Center for Environmental Health, Division of Laboratory Services (CDC-NCEH-DLS), which supports a reference system for the measurement of total glycerides in clinical samples. SRM 1595 was also used by analytical reference laboratories that contribute to the Cholesterol Reference Method Laboratory Network, a specialized group that works with analytical equipment manufactures and other laboratories to assess accuracy of clinical tests.

SRM 1595 was originally certified in 1983; the sales history from the earliest readily accessible records in 1990 to the final sales in late 2018 is displayed in Fig. 2.

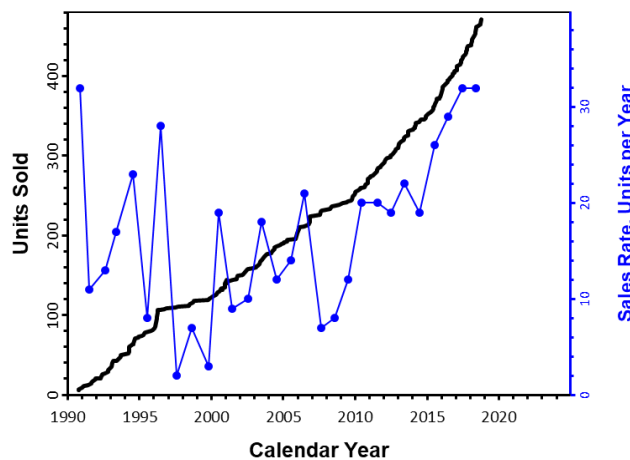


Fig. 2. Sales History of SRM 1595.

The thick black line depicts the cumulative distribution of sales as a function of the order date; it is plotted using the “Units Sold” axis at the left of the plot. The thin blue line depicts the total units sold per year; it is plotted using the “Sales Rate, Units per Year” axis to the right of the graph. There are no accessible records of SRM sales prior to August 1990.

The proportion of sales to customers in the United States of America (USA), Europe, Asia, and the rest of the world are displayed in Fig. 3. Over 80 % of the 471 units of SRM 1595 that have been sold since 1990 have been purchased by customers within the USA.

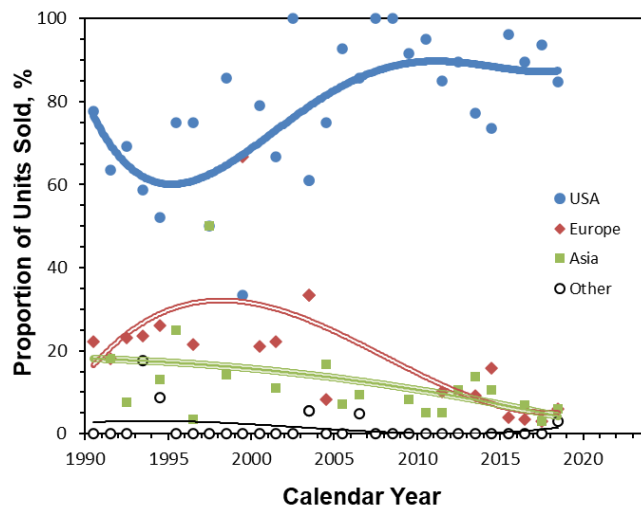


Fig. 3. Location of Customers for SRM 1595 Tripalmitin.

The solid circles and the thick polynomial trendline display the proportion of sales to customers within the USA from the onset of currently accessible electronic records in 1990 to the date of the last unit sold in 2018. Solid diamonds and the double-line polynomial trendline display the proportion of units sold to customers in Europe (including the United Kingdom); solid squares and the triple-line polynomial trendline display the proportion sold to customers in Asia. The open circles and thin polynomial trendline display the proportion of units sold to customers elsewhere.

The identity of tripalmitin in SRM 1595a has been established through appropriate nuclear magnetic resonance spectroscopy (NMR) and high-resolution mass spectrometry (HRMS) techniques. The tripalmitin purity has been established through calibration to a material whose purity was assigned by calibration to NIST PS1 Primary Standard for quantitative NMR (Benzoic Acid) via a primary ratio method [3] that uses quantitative proton nuclear magnetic resonance spectroscopy with an internal standard ($^1\text{H-qNMR}_{\text{IS}}$) [6,7]. The very low water content of the tripalmitin has been established using thermogravimetric analysis (TGA). The homogeneity of the SRM 1595a units has been established through the $^1\text{H-qNMR}_{\text{IS}}$ and TGA analyses.

Measurement results calibrated via SRM 1595a can be established as metrologically traceable to the International System of Units (SI). SI-traceability is now recognized as essential to enabling comparison of clinical measurements across time and place [4,5].

2. Production

Two plastic screw-top jars (white, opaque) containing bulk neat tripalmitin were acquired from NuChek Prep, Inc. (Elysian, MN, USA), the manufacturer that supplied the SRM 1595 material. While from the same production lot, “Jar 2” which contained about 200 g of neat tripalmitin was delivered about three months after “Jar 1” which contained about 300 g of the neat material. The jars were stored at a temperature of -20 °C until acceptance analysis could be performed.

Following acceptance, the materials in the two jars were bottled separately. The materials were not blended to minimize the potential for contamination. A total of 240 units were bottled by the Office of Reference Materials at its facilities in Gaithersburg, MD. The first 98 units of the filling sequence contain material from “Jar 2”; units 99 through 240 contain material from “Jar 1”. Each unit consists of approximately 2 g of neat tripalmitin powder in an amber glass bottle sealed with a polytetrafluoroethylene-lined polymer screwcap.

3. Material Suitability Assessment

3.1. Materials

A tecnazene (1,2,4,5-tetrachloro-3-nitrobenzene) material of known purity was used as an internal standard. The chemical structure of tecnazene is displayed in Fig. 4. The purity of this material had been established at NIST using ^1H -qNMR_{IS} with NIST PS1 Benzoic Acid [6,7] as the internal standard. This material is stored at room temperature in a desiccator.

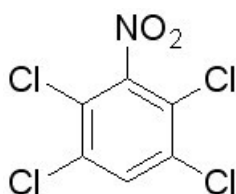


Fig. 4. Chemical Structure of Tecnazene.

Samples for qNMR analysis were solvated with CDCl_3 (chloroform-*d*) from Cambridge Isotope Laboratories.

3.2. Sample Preparation

Preparation of samples for $q^1\text{H}$ -NMR analysis and sample mass determinations were performed in accordance with established protocols.

Glassware used during sample preparation was rinsed with acetone, methanol, ethanol, and distilled water and baked in a furnace at 450 °C. Sample preparation was performed under light from a single white incandescent bulb. Clean Bruker 600 MHz NMR tubes (5 mm internal diameter, 7-inch length) were used.

Neat material masses of (4 to 10) mg were determined using a calibrated ultra-microbalance (Mettler Toledo XPR2U, Columbus, OH). Approximately 0.7 mL of CDCl_3 was used to dilute the samples. To facilitate total dissolution, samples were sonicated and vortexed. Care was taken to ensure complete dissolution and that no crystals of the neat materials adhered to the weigh bottle walls.

3.3. Instrumentation and Signal Analysis

Experimental NMR data was acquired by a Bruker Avance II 600 MHz spectrometer equipped with a 5-mm double resonance broadband probe with inverse coil configuration to optimize ^1H observation. The system was operated using Topspin (Version 3.2) software. The ^1H experimental analyses, subsequent data processing and chemical mass fraction purity determinations were performed according to established protocols.

One dimensional ^1H NMR experiments were conducted using 90-degree excitation pulse widths, without ^{13}C decoupling. All experiments were conducted at 298 °K. For each analysis, 64 acquired data scans were averaged, 2 dummy scans performed, the spectral sweep width was set to 20.0276 ppm, and the transmitter frequency offset for the ^1H (O1) channel was set to

6.175 ppm. Data acquisition time was 5.4525952 s for each scan to generate an FID with 131072 data points. Signal digitization was performed using TopSpin default 'digital' mode. The spin lattice relaxation time (T1) for all analyzed tripalmitin and tecnazene ^1H resonances was determined using magnetization inversion recovery NMR experiments. The longest T1 among relevant resonances for all sample compositions was 1.4 s. The recycle delay, D1, was set to 80 s, allowing approximately 99.999 % recovery of the net magnetization equilibrium position between scans.

An additional method of data processing was performed using MestreNova (MNOVA) Version 14.1.2 NMR spectral analysis software. After phasing and using an automated multi-point baseline correction procedure, the 'Automatic Peak Picking' functionality using 'Global Spectral Deconvolution' (GSD, using 10 fitting cycles) was implemented to fit lines to all observed peaks in the spectrum. Each of the fitted peaks across the regions of interest were categorized as either "Compound", corresponding to resonances of tripalmitin and tecnazene, or "Impurity". Calculation of integrals for manually assigned spectral regions containing the peaks of interest was performed in MestreNova using the 'Edited Sum' integral calculation method. This functionality subtracts the area under the GSD-fit peaks assigned peak type "Impurity" from the integral of the respective tripalmitin or tecnazene peak calculated using the Fourier transformed FID data.

3.4. Identification

3.4.1. NMR Spectroscopy

The structure of tripalmitin in the bulk candidate material for SRM 1595a was verified via ^1H , ^{13}C , ^1H - ^{13}C heteronuclear single quantum coherence (HSQC), and ^1H - ^{13}C heteronuclear multiple bond correlation (^1H - ^{13}C HMBC) NMR experiments. The ^1H -NMR spectrum with peak assignments is displayed in Fig. 5.

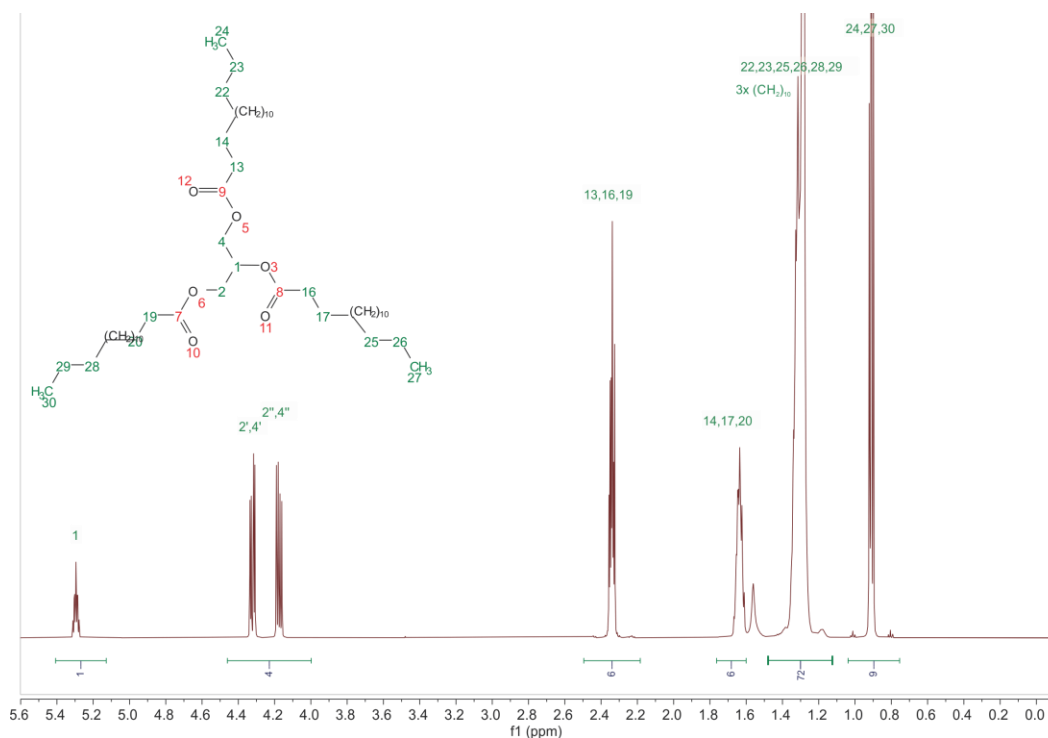


Fig. 5. Exemplary ¹H Spectrum of Bulk Candidate SRM 1595a Tripalmitin in CDCl₃.

The tripalmitin peaks and the lone tecnazene peaks that were evaluated for purity assessments are summarized in Table 1.

Table 1. Summary of ¹H-NMR Spectrum Peaks Evaluated for qNMR Purity Analysis.

	chemical shift	peak type	¹ H structural moiety	proton multiplicity	T1 (s)
tripalmitin	5.1 to 5.5 ppm	multiplet	1	1	1.4
	3.9 to 4.6 ppm	two split doublets	2,4	2	0.6
	2.2 to 2.5 ppm	multiplet	13,16,19	6	0.8
tecnazene	7.5 to 8.0 ppm	singlet		1	1.8

The expanded-scale ¹H-NMR signals for SRM 1595 and the two jars of the bulk SRM 1595a candidate material are displayed in Fig. 6 for the tripalmitin moieties 2 and 4 (panel a) and moieties 13, 16, 19 (panel b). Fewer impurities are observed across these ¹H spectral regions for the bulk candidate materials than for SRM 1595.

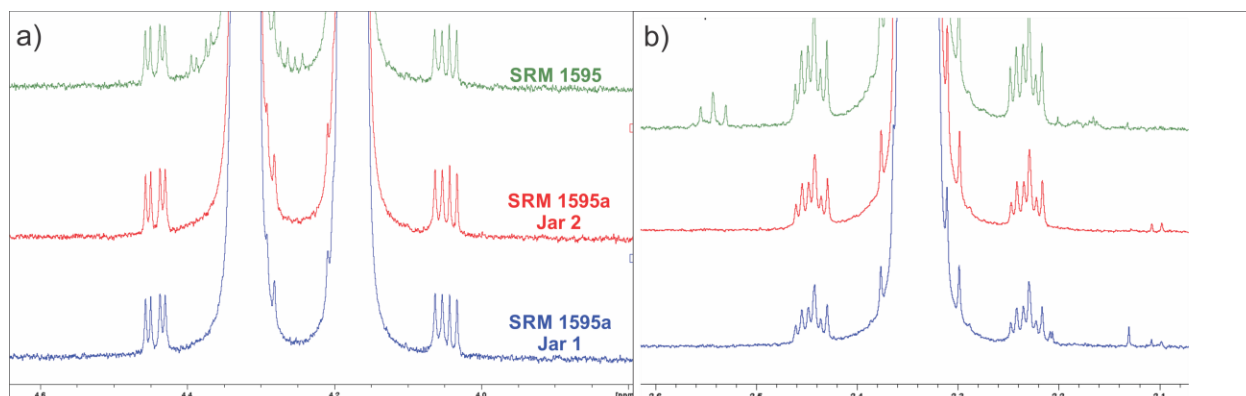


Fig. 6. Comparison of ^1H Spectral Regions for SRM 1595 and SRM 1595a.

Panel a) Chemical shift interval centered on the two split doublets of moieties 2 and 4.

Panel b) Chemical shift interval centered on the multiplet of moieties 13, 16, and 19.

The ^1H - ^{13}C HSQC spectrum is displayed in Fig. 7; the ^1H - ^{13}C HMBC spectrum is displayed in Fig. 8. All expected peaks were observed and no unexpected peaks were observed above baseline noise levels.

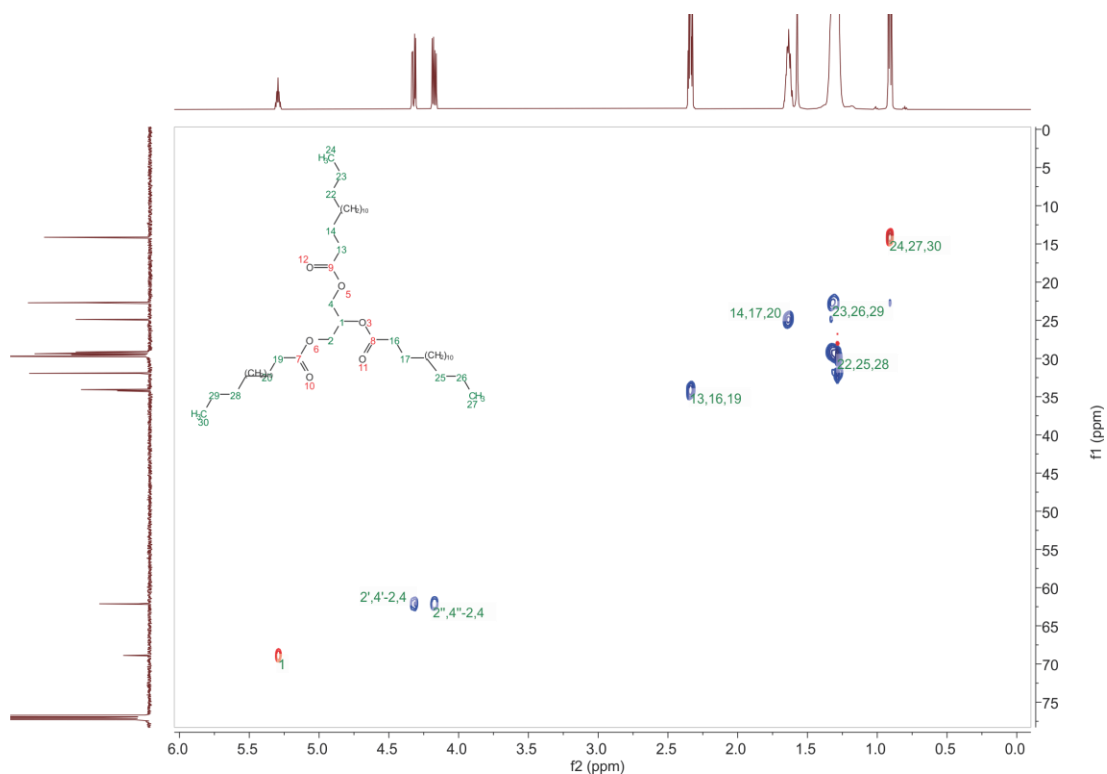


Fig. 7. ^1H - ^{13}C HSQC Spectrum of Bulk Candidate SRM 1595a Tripalmitin in CDCl_3 with ^1H - ^{13}C Correlation Assignments.

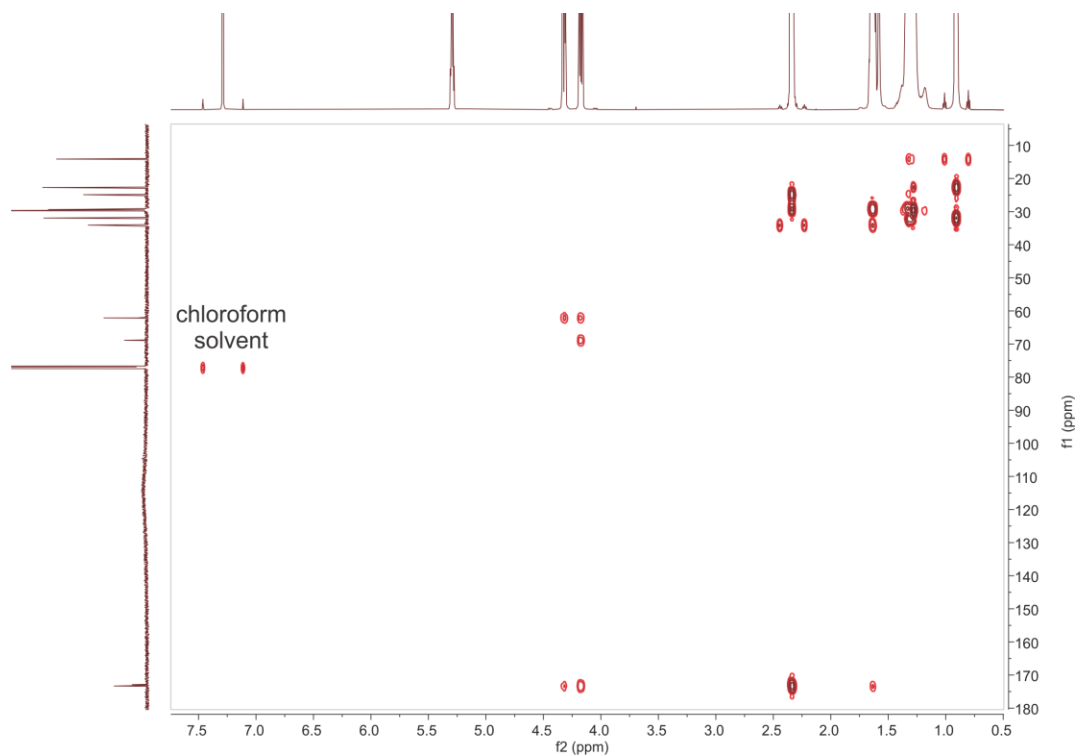


Fig. 8. ^1H - ^{13}C HMBC Spectrum of Bulk Candidate SRM 1595a Tripalmitin in CDCl_3 .

3.4.2. High Resolution Mass Spectral Evaluation

Samples of the bulk SRM 1595a tripalmitin material were delivered to the U.S. Centers for Disease Control and Prevention (CDC) in Atlanta, GA for analysis by experts in the National Center for Environmental Health, Division of Laboratory Sciences. The aim of the analysis was to screen for structurally related fatty acid and triglyceride impurities that are not discernable using NMR. This was accomplished using direct infusion electrospray ionization (ESI) coupled to high resolution mass spectrometry (HRMS) and tandem mass spectrometry.

MS data were acquired in March 2022 using a Thermo Scientific Orbitrap Eclipse Tribrid Mass Spectrometer equipped with an Ion Max NG heated ESI source, operated in positive ionization mode. A $50\ \mu\text{g}/\text{mL}$ solution of SRM 1595a was prepared in a solvent comprising chloroform and methanol in a ratio of 2:1 (volume fraction). Once diluted, $20\ \mu\text{L}$ of a $0.1\ \text{mol}/\text{L}$ ammonium acetate solution in water was added to the tripalmitin sample to encourage formation of ammonium adduct ion types. Aliquots of this solution were directly infused for analysis by HRMS. The identity of the tripalmitin primary component was verified. The spectrum also showed small quantities of other ions; however, further investigation by the CDC determined that the tripalmitin material did not contain appreciable quantities of other fatty acids or triglyceride impurities that might interfere with the quantified ^1H -NMR peak of tripalmitin.

3.5. Quantitative Analysis

Measured values of mass fraction (g/g), w_P , of tripalmitin in samples of the bulk SRM 1595a candidate material were determined via $q^1\text{H-NMR}_{\text{IS}}$ using the following measurement function:

$$w_p = \left(\frac{N_I}{N_P}\right) \times \left(\frac{M_P}{M_I}\right) \times \left(\frac{A_P}{A_I}\right) \times \left(\frac{m_I}{m_C}\right) \times P_I \quad (1)$$

where: N_p = ^1H multiplicity (# H/peak) of the integrated tripalmitin peak,
 N_I = ^1H multiplicity (# H/peak) of the integrated tecnazene internal standard peak,
 M_p = relative molar mass (molecular weight, g/mol) of tripalmitin,
 M_I = relative molar mass (molecular weight, g/mol) of tecnazene,
 A_p = integral of the tripalmitin ^1H peaks,
 A_I = integral of the tecnazene ^1H peak,
 m_C = mass (g) of sampled neat tripalmitin material,
 m_I = mass (g) of tecnazene, and
 P_I = purity (%) of the tecnazene internal standard.

3.5.1. Experimental Design

Two sets of four qNMR analysis sample replicates (eight in total) were prepared. For each set, two samples were collected from each of the two jars. A diagram of the balanced nested design scheme for q ^1H -NMR experiments is shown in Fig. 9.

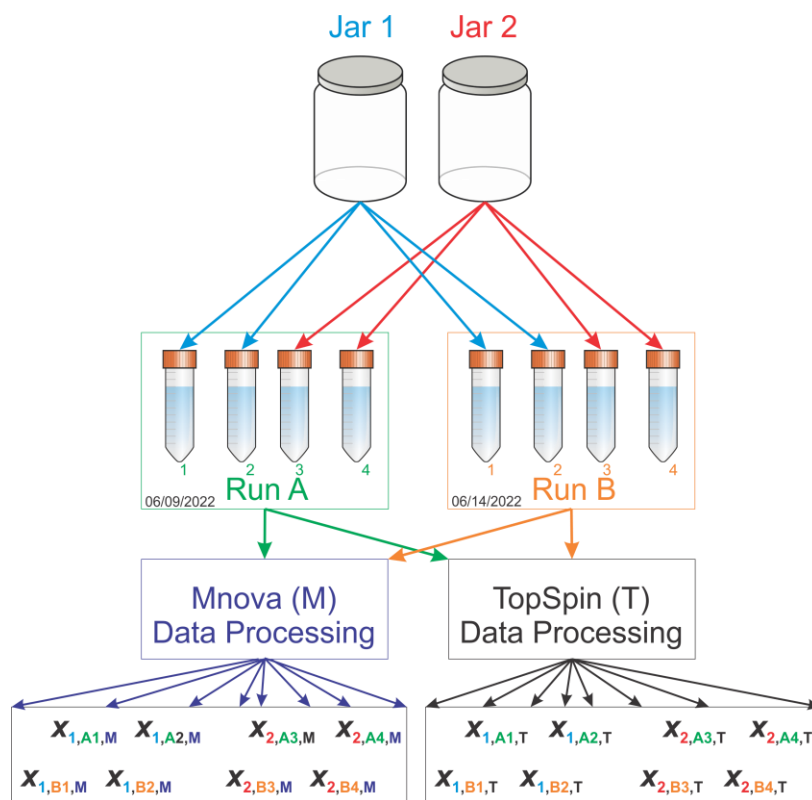


Fig. 9. Experimental Design for the Analysis of Bulk Candidate SRM 1595a Tripalmitin Purity.

3.5.2. Spectral Integral Selection

Processing of NMR data to determine purity values was conducted using both the MNova and TopSpin NMR software. As displayed in Fig. 10, measured purity values determined for each replicate from each of the three tripalmitin integral regions in Table 1 were plotted against analysis run order. There is a moderate correlation of -0.72 between run order and the MNova results for the multiplet for moiety 1 at 5.3 ppm, suggesting that the area under these peaks changes over time or that there might be some effect over time impacting consistency in integral determinations. However, there is no correlation with the Topspin results.

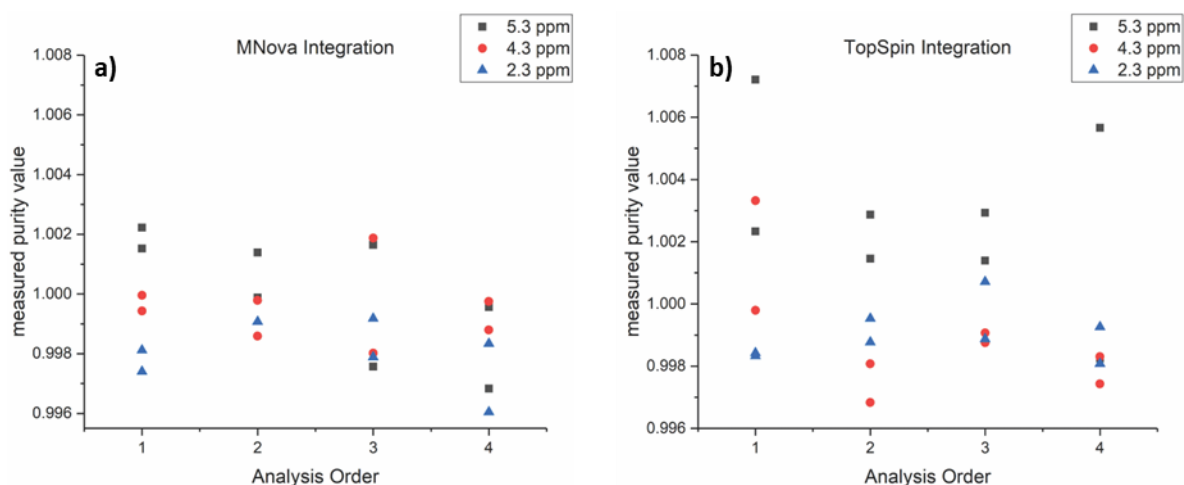


Fig. 10. Purity Values Calculated Using Integrals for Three ^1H Spectral Regions.

Both panels display measured purity values as functions of analysis order in the two Runs. Square symbols represent results calculated using the moiety 1 multiplet integral; circles represent results from the moiety 2,4 split doublets; triangles represent results from the moiety 13, 16, 19 multiplet.

Panel a) Purity values estimated using integrals provided by the MNova software.

Panel b) Purity values estimated using integrals provided by the TopSpin NMR software.

While the correlation may be spurious, purity values calculated using integrals of the 5.3 ppm peak are generally higher than those from the other two peaks. It was initially considered that this might indicate some small proportion of the integral for ^1H moiety 1 is attributable to a structurally related impurity component, such as another glyceride. However, the overall precision of purity values determined from this peak is notably less than that for the other two peaks. The distributions of the purity values grouped by integrated spectral region are displayed in Fig. 11.

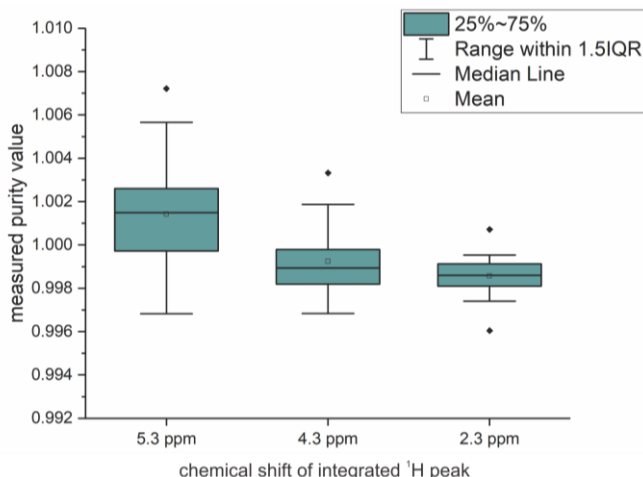


Fig. 11. Purity Value Distributions for Integrals From Three ^1H Spectral Regions.

Furthermore, the precision of results calculated using integrals of the broad peak region centered at 4.3 ppm was lower than those using integrals of the peak centered at 2.3 ppm. This suggested that tripalmitin peak integration and overlapping impurity peak adjustments are more consistently performed for the narrower peak region centered at 2.3 ppm. For these reasons, measured purity values calculated using integrals of the 2.3 ppm peak are considered the most reliable.

3.5.3. Sample Purity Estimates

The multiplicity of the 13,16,19 moiety of the peak region centered at 2.3 ppm is $N_p = 6$. The multiplicity of the tecnazene peak is $N_i = 1$.

Using the authoritative molecular weight calculator implemented by the IUPAC Commission on Isotopic Abundances and Atomic Weights [8], the relative molar masses and their standard uncertainties for tripalmitin ($\text{C}_{51}\text{H}_{98}\text{O}_6$) and tecnazene ($\text{C}_6\text{HCl}_4\text{NO}_2$) are $M_p = (807.319 \pm 0.031) \text{ g/mol}$ and $M_i = (260.833 \pm 0.013) \text{ g/mol}$, respectively.

The purity of the tecnazene internal standard and its standard uncertainty was determined at NIST to be $P_i = (0.9979 \pm 0.0009) \text{ g/g}$.

The values of the measured parameters for the Jar 1 and Jar 2 samples are listed in Table 2. The estimated sample-specific purities are reported in Table 3. For the purpose of this suitability analysis, the standard uncertainties of the estimates have not been calculated.

Table 2. Measured Parameter Values for Jar 1 and Jar 2 Samples.

Source	Parameter	Units	Sample 1	Sample 2	Sample 3	Sample 4
Jar 1	m_c	mg	4.6579	4.2786	4.1872	4.5993
	m_i	mg	6.9502	6.593	5.7297	6.8225
	A_p/N_p (NMova)	planar units	126327	117152	118331	134030
	A_i/N_i (NMova)	planar units	583185	557984	501330	614528
	A_p/N_p (TopSpin)	planar units	129502097	120070456	121470454	137651367
	A_i/N_i (TopSpin)	planar units	597659165	572055631	514152186	630841615
Jar 2	m_c	mg	7.4575	7.0558	5.4466	7.7779
	m_i	mg	9.9637	6.266	6.6827	4.6193
	A_p/N_p (NMova)	planar units	132600	147042	128843	145697
	A_i/N_i (NMova)	planar units	547534	403921	489206	268223
	A_p/N_p (TopSpin)	planar units	136101386	151082334	132379202	149827068
	A_i/N_i (TopSpin)	planar units	561133545	414633843	502137722	275311808

Table 3. Tripalmitin Purity Determined Using Integrals of the 2.3 ppm Spectral Interval.

Material	Run	Sample	Replicate	x_{MNova}	$x_{TopSpin}$
Jar 1	A	Jar 1-1	1	0.9984	0.9981
		Jar 1-2	2	0.9988	0.9991
	B	Jar 1-3	1	0.9983	0.9974
		Jar 1-4	2	0.9995	0.9991
Jar 2	A	Jar 2-1	3	0.9989	0.9979
		Jar 2-2	4	0.9981	0.9962
	B	Jar 2-3	3	1.0007	0.9992
		Jar 2-4	4	0.9993	0.9983

3.5.4. Influence of Run, Jar, Sample, and Software Factors

Analyses of variance (ANOVA) were conducted via Excel on the results in Table 3 to evaluate factors of the multi-stage nested experiment design. Table 4 lists the data groupings and the two-way ANOVA assessment of between-Run and -replicate variance. Table 5 lists the data groupings and the two-way ANOVA assessment of between-Jar and -replicate variance. Table 6 lists the data groupings and the one-way ANOVA assessment of between-sample. Table 7 lists the data groupings and the one-way ANOVA assessment of between-software variance. The three panels of Fig. 12 provide graphical assessments of the between-Run, -Jar, and -software factors. None of the factors are significant at the 0.05 statistical significance threshold. The lack of significant between-jar or between-sample effects suggest that the bulk tripalmitin is sufficiently homogenous for 5 mg to 10 mg sample sizes with respect to the degree of variation observed in the q^1H -NMR analyses.

Table 4. Two-Way ANOVA Assessment of Between-Run and Between-Replicate Variance.

Run ^a	BtwRep 1 ^b	BtwRep 2 ^b	BtwRep 3 ^b	BtwRep 4 ^b
A	0.9984	0.9988	1.0007	0.9993
	0.9981	0.9991	0.9992	0.9983
B	0.9983	0.9995	0.9989	0.9981
	0.9974	0.9991	0.9979	0.9962

Source	SS	df	MS	F	P-value	F crit
Between Run	2.62994E-06	1	2.62994E-06	4.73	0.061	5.32
Columns	5.01145E-06	3	1.67048E-06	3.00	0.094	4.07
Interaction	2.87078E-06	3	9.56928E-07	1.72	0.23	4.07
Within	4.44503E-06	8	5.55628E-07			
Between replicate	7.88223E-06	6	1.3137E-06	0.42	0.84	
Total	1.49572E-05	15				

- a Rows within Run represent between-Run replication, treated as values determined from the same spectrum using the two different NMR processing software packages.
- b Between-Run replicates, ordered by sample sequence within each Jar (identical to the “Replicate” identified in Table 3).

Table 5. Two-Way ANOVA Assessment of Between-Jar and Between-Replicate Variance.

Jar ^a	WthRep 1 ^b	WthRep 2 ^b	WthRep 3 ^b	WthRep 4 ^b
1	0.9984	0.9988	0.9983	0.9995
	0.9981	0.9991	0.9974	0.9991
2	0.9989	0.9981	1.0007	0.9993
	0.9979	0.9962	0.9992	0.9983

Source	SS	df	MS	F	P-value	F crit
Between Run	2.12561E-09	1	2.12561E-09	0.0038	0.95	5.32
Columns	2.76438E-06	3	9.21461E-07	1.65	0.25	4.07
Interaction	7.74566E-06	3	2.58189E-06	4.65	0.037	4.07
Within	4.44503E-06	8	5.55628E-07			
Between replicate	1.05100E-05	6	1.75167E-06	0.32	0.91	
Total	1.49572E-05	15				

- a Rows within Jar represent replication, treated as values determined from the same spectrum using the two different NMR processing software packages.
- b Within-Run replicates, ordered by analysis sequence within each Run.

Table 6. One-Way ANOVA Assessment of Between-Sample Variance.

	Run A	Run B
	0.9981	0.9974
	0.9991	0.9991
	0.9992	0.9979
	0.9983	0.9962
	0.9984	0.9983
	0.9988	0.9995
	1.0007	0.9989
	0.9993	0.9981

Source	SS	df	MS	F	P-value	F crit
Between Run	2.62994E-06	1	2.62994E-06	2.99	0.11	4.60
Within replicates	1.23273E-05	14	8.80518E-07			
Total	1.49572E-05	15				

Table 7. One-Way ANOVA Assessment of Between-Software Variance.

	MNova	TopSpin
	0.9981	0.9984
	0.9991	0.9988
	0.9992	1.0007
	0.9983	0.9993
	0.9974	0.9983
	0.9991	0.9995
	0.9979	0.9989
	0.9962	0.9981

Source	SS	df	MS	F	P-value	F crit
Between Run	2.79762E-06	1	2.79762E-06	3.23	0.094	4.60
Within replicates	1.21596E-05	14	8.68541E-07			
Total	1.49572E-05	15				

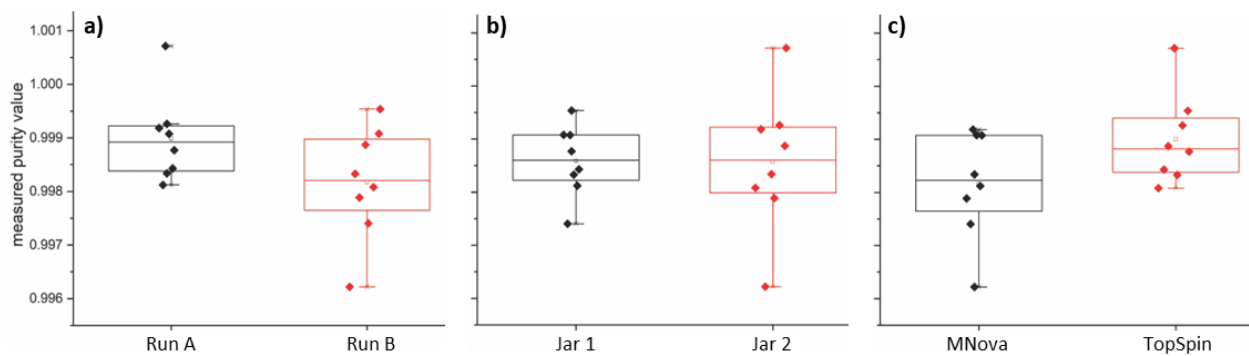


Fig. 12. Boxplots of Purity Values Comparing Run, Jar, and Software Factors.

All panels contrast two groupings of the measured purity values:
 Panel a) Purity values grouped by Run (Run A, Run B).
 Panel b) Purity values grouped by Jar (Jar 1, Jar 2).
 Panel c) Purity values grouped by software (MNova, TopSpin).

3.5.5. Influence of $^1\text{H-NMR}$ Analysis Order

While Run, Jar, sample and software do not significantly influence the measured purity values, as shown in Fig. 13 the position of samples in the $^1\text{H-NMR}$ analysis run order does.

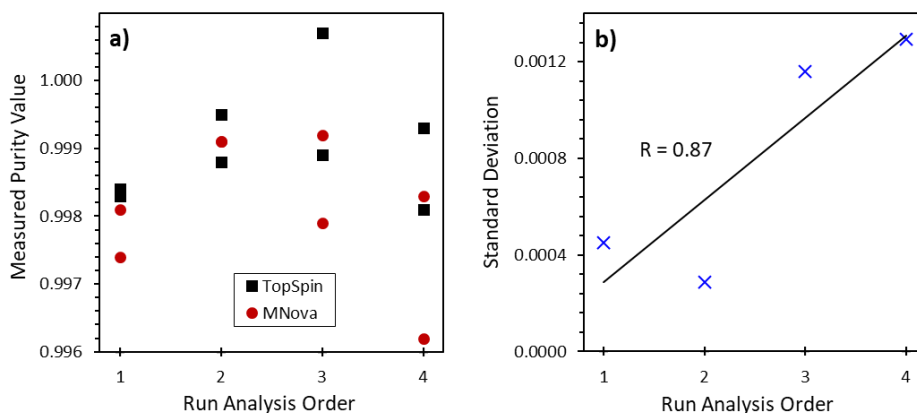


Fig. 13. Measured Purity Values and Standard Deviation as Functions of Analysis Order.

Panel a) Purity values grouped by the $^1\text{H-NMR}$ analysis order, 1 to 4. Square symbols represent results derived from the TopSpin integrals; circles represent results from the MNova integrals.

Panel b) standard deviations of the four values within each Run analysis order, plotted as a function of Run analysis order.

The correlation between the standard deviation and the order in which the samples were analyzed is 0.87. Given the experimental design (Fig. 9), this could be attributable to the time lapse between sample dilution and experiment completion (lability) and/or to greater heterogeneity of the Jar 2 material. Since 1) the former effect is relatively common, 2) no significant between-Jar or between-replicate effect was detected, and 3) the bulk containers contain material from the same production batch, the amount of time between sample dilution and completion of the $^1\text{H-NMR}$ analysis should be constrained to no more than 4.5 hours. It was noted that the possibility of greater variation in analysis of samples from Jar 2 should also be explored. The observed *statistical* correlation was kept in mind when evaluating variation in measured purity from samples collected across the bottling order of the lot.

3.5.6. Estimated Purity

The mean (μ) and standard deviation of the mean of the measured tripalmitin purity values ($n = 16$, $df = 15$) are 0.9986 g/g and 0.0003 g/g, respectively. The purity of the bulk tripalmitin material is estimated to be attributable to the value interval [0.9961, 1] g/g, corresponding to an approximately 95 % level of confidence. For determination of this interval, two components of uncertainty were calculated as standard deviations of measured values, s , treated as representative estimates of the standard deviation of the population of plausible values, σ . A combined standard uncertainty, u , was approximated by combining the between-replicate standard deviation, s_b , and within-sample replicate standard deviation, s_w (repeatability via results determined using different NMR software), calculated using the one-way ANOVA results in Table 8.

Table 8. One-Way ANOVA Assessment of Between-Software Variance.

Replicate	Sample 1	Sample 2	Sample 3	Sample 4	Sample 5	Sample 6	Sample 7	Sample 8
1 (MNova)	0.9981	0.9991	0.9992	0.9983	0.9974	0.9991	0.9979	0.9962
2 (TopSpin)	0.9984	0.9988	1.0007	0.9993	0.9983	0.9995	0.9989	0.9981

Source	SS	df	MS	F	P-value	F crit
Between replicates	1.05994E-05	7	1.5142E-06	2.69	0.095	3.50
Within replicates	4.50500E-06	8	5.6312E-07			
Total	1.05994E-05	7	1.5142E-06			

For this analysis, s_w and s_b are treated as fit-for-purpose approximations of the uncertainties associated with the $q^1\text{H-NMR}$ analysis and uncertainties arising from sampling of the bulk material. These estimates were calculated as:

$$s_w^2 = MS_{\text{within}} \quad (2)$$

$$s_b^2 = \text{MAX} \left(\frac{MS_{\text{between}} - MS_{\text{within}}}{n_r}, 0 \right) \quad (3)$$

where MS_{within} is the “within-replicates” mean square value in Table 8, and MS_{between} is the “between-replicates” mean square value, n_r is the number of analyses per replicate (here, $n_r=2$, one value per software), and MAX is the function “take the maximum of the series of values.” The values for s_b and s_w are calculated as 0.00069 g/g and 0.00075 g/g, respectively.

The standard uncertainty of the purity estimate is a combination of these two components:

$$u = \sqrt{n_r s_b^2 + s_w^2} = \sqrt{2 \times 0.00069^2 + 0.00075^2} \cong 0.00126 \text{ g/g} \quad (4)$$

The expanded uncertainty, U , was calculated as:

$$U = k \times u = 2 \times 0.00126 \cong 0.0025 \text{ g/g} \quad (5)$$

where the coverage factor was treated as $k = 2$. The value interval corresponding to an approximate 95 % level of confidence was determined as:

$$\begin{aligned} [\mu - U, \text{MIN}(\mu + U, 1)] &= [0.9986 - 0.0025, \text{MIN}(0.9986 - 0.0025)] \\ &= [0.9961, \text{MIN}(1.0011, 1)] = [0.9961, 1] \text{ g/g} \end{aligned} \quad (6)$$

where MIN is the function “take the minimum of the series of values.”

3.5.7. Conclusions

The bulk candidate SRM 1595a material is confidently identified as tripalmitin.

The Jar 1 and Jar 2 materials are sufficiently similar and homogeneous in tripalmitin content (mass fraction) for 5 mg to 10 mg samples.

Given that the certified value of purity of SRM 1595 Tripalmitin is $(99.5 \pm 0.2) \%$, the estimated $[0.9961, 1.0000]$ g/g purity of the bulk candidate SRM 1595a tripalmitin material investigated in this study has been demonstrated to be fit for the purpose of developing candidate SRM 1595a Tripalmitin.

4. ^1H -NMR Purity and Homogeneity Assessment

After bottling, ten units of SRM 1595a were sampled and analyzed by qNMR to determine the mass fraction of tripalmitin in the SRM. Moisture analysis using Karl Fischer titration and thermogravimetric analysis was conducted using the same 10 units to confirm the purity value and to verify that the material is sufficiently homogenous. Additionally, lipid analysis experts of the Centers for Disease Control verified the absence of structurally similar lipid and fatty acid impurity components that could have influenced the NMR purity analysis. This impurity survey was conducted using ESI-HRMS.

4.1. Materials

From the 240 units of the production lot, ten were sampled for characterization of SRM 1595a. The units sampled were from across the bottling order. Table 9 lists the units evaluated.

Table 9. Sampling Scheme

Jar	Number of Units Evaluated	Fill Order of Units Evaluated
2	4	1, 30, 60, 90
1	6	99, 120, 150, 180, 210, 240

A tecnazene (1,2,4,5-tetrachloro-3-nitrobenzene) material of known purity was used as an internal standard. The chemical structure of tecnazene is displayed in Fig. 4. The purity of this material had been established at NIST using ^1H -qNMR_{IS} with NIST PS1 Benzoic Acid [6,7] as the internal standard. This material is stored at room temperature in a desiccator.

Samples for qNMR analysis were solvated with CDCl_3 (chloroform-*d*) from Cambridge Isotope Laboratories.

4.2. Sample Preparation

A total of ten qNMR samples were prepared, one sample from each unit. Sample preparation was performed in the dark using a lamp with a white incandescent bulb. Samples were weighed, dissolved, and analyzed one at a time to mitigate any issues related to tripalmitin instability over time. Sample mass determinations and preparation of samples for q ^1H -NMR analysis were performed in accordance with established protocols.

Glassware used during sample preparation was rinsed with acetone, methanol, ethanol, and distilled water and baked in a furnace at 450 °C. Clean Bruker 600 MHz NMR tubes (5 mm internal diameter, 7-inch length) were used.

Neat material masses of approximately (5 to 11) mg were determined using a calibrated ultra-microbalance (Mettler Toledo XPR2U, Columbus, OH). Approximately 0.7 mL of CDCl_3 was used to dilute the samples. Samples were then sonicated several times and then vortexed to achieve complete dissolution while ensuring that no crystals of the neat materials adhered to the weigh bottle walls.

4.3. Analysis

4.3.1. ^1H -qNMR_S Evaluation

Experimental NMR data was acquired by a Bruker Avance II 600 MHz spectrometer equipped with a 5-mm double resonance broadband probe with inverse coil configuration to optimize ^1H observation. The system was operated using Topspin (Version 3.2) software. The ^1H experimental analyses, subsequent data processing and chemical mass fraction purity quantifications were performed in accordance with established protocols.

One dimensional ^1H NMR experiments were conducted using 90-degree excitation pulse widths, with ^{13}C decoupling (zgig). All experiments were conducted at 298 °K. For each analysis, 64 acquired data scans were averaged, 16 dummy scans performed, the spectral sweep width was set to 20.0276 ppm, and the transmitter frequency offset for the ^1H (O1) channel was set to 6.175 ppm. Data acquisition time was 5.45 s for each scan to generate an FID with 131072 data points. Signal digitization was performed using TopSpin 'baseopt' mode. The spin lattice relaxation time (T1) for all analyzed tripalmitin and internal standard ^1H resonances was determined using magnetization inversion recovery NMR experiments. The longest T1 among relevant resonances for all sample compositions was 1.8 s. The relaxation delay, D1, was set to 80 s, ensuring approximately 99.999 % recovery of the net magnetization equilibrium position between scans.

The tripalmitin identity of the packaged SRM 1595a units, established for the bulk material as described in Section 3.4, was verified via ^1H -NMR as demonstrated in Fig. 14.

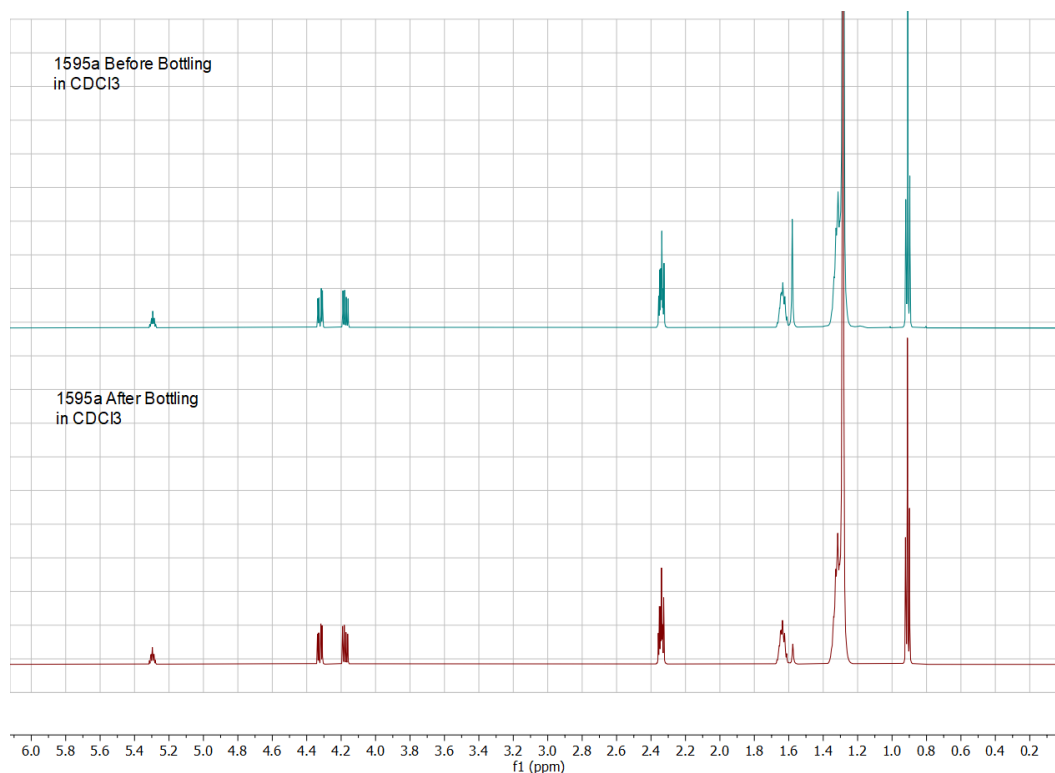


Fig. 14. Comparison of the Candidate SRM 1595a Tripalmitin ^1H Spectra Before and After Bottling.

Measured mass fraction purity values were determined via $q^1\text{H-NMR}_{\text{IS}}$ using Eq. (1), the measurement function described in Section 3.4.2, with the (2.2 to 2.5) ppm integral for the ^1H tripalmitin moiety (13, 16, 19) of multiplicity $N_p = 6$ and the (7.5 to 8.0) ppm tecnazene singlet of multiplicity $N_t = 1$. These multiplicities are considered to have standard uncertainties equal to 0. The integrals of the tripalmitin peak centered at 2.3 ppm were selected for quantitation because they were deemed more reliable, free of overlapping peaks and spectral interferences, and more precisely determined than those for the other peaks (see Section 3.5.2). An example spectrum demonstrating the integration regions is shown in Fig. 15. Two samples were evaluated per measurement session day.

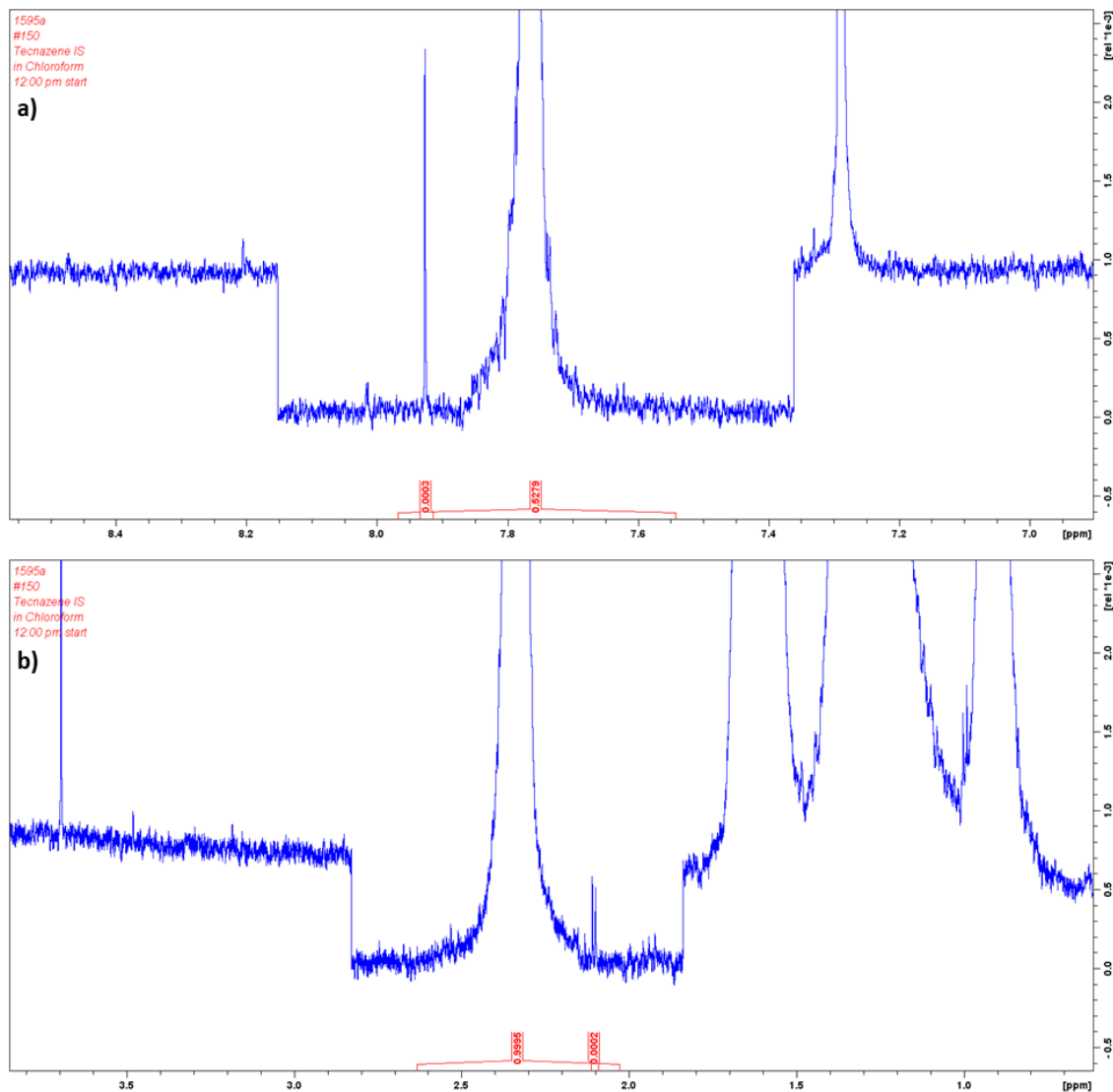


Fig. 15. Integration Regions Used to Calculate Peak Areas.

The blue traces represent exemplar NMR signals in the spectral regions of interest following manual phase adjustment and baseline correction. The red curves just above the horizontal axis denote the integration intervals. The very narrow spikes in the traces likely arise from minor impurities.

Panel a) Spectral region used for tecnazene.

Panel b) Spectral region used for tripalmitin.

For each variable term of Eq. 1, the measurement data for each sample was treated as having a $N(\mu, \sigma)$ normal distribution. The means, μ , and their standard uncertainties, $\sigma = u(\mu)$, were evaluated as follows:

- The proton multiplicity of the tripalmitin signal is $N_P = 6$ with $u(N_P) = 0$. The multiplicity of the tecnazene signal is $N_I = 1$ with $u(N_I) = 0$.
- Using the authoritative molecular weight calculator implemented by the IUPAC Commission on Isotopic Abundances and Atomic Weights [8], the relative molar mass for tripalmitin ($C_{51}H_{98}O_6$) and its standard uncertainty is $M_P = 807.319$ g/mol with $u(M_P) = 807.319$ g/mol 0.031) g/mol. The relative molar mass and standard uncertainty for tecnazene ($C_6HCl_4NO_2$) is $M_I = 260.833$ with $u(M_I) = 0.013$ g/mol.
- The tripalmitin and tecnazene integrated areas, A_P and A_I , are experimental measurements. Based on experience, the expected relative standard uncertainty of the tripalmitin integrals is $u(A_P)_{rel} = 0.15$ %. The expected relative standard uncertainty of the tecnazene integrals is $u(A_I)_{rel} = 0.05$ %.
- The sample and internal standard masses, m_C and m_I , are experimental measurements. From the calibration certificate for the ultra-microbalance used, the expected standard uncertainty for masses weighed, here $u(m_C)$ and $u(m_I)$, is 0.0005 mg.
- The purity of the tecnazene internal standard was determined at NIST to be $P_I = 0.9979$ g/g with standard uncertainty $u(P_I) = 0.0009$ g/g.

The values of the measured parameters for the ten samples are listed in Table 10, along with sample-specific purities estimated from direct application of Eq. (1). The information is listed in order of qNMR analysis. Since the multiplicities are considered as exact, for convenience they are included in the values for the integrated areas.

Table 10. Sample-Specific Measurement inputs and Purity Estimates.

Order		Areas, planar units		Masses, mg		Purities, g/g	
Analysis	Fill	A_P/N_P	A_I/N_P	m_C	m_I	w_P	$u(w_P)$
1	210	270842992	1479459416	5.8893	10.3966	0.9982	0.0023
2	120	282776837	1422374090	6.4043	10.4184	0.9989	0.0023
3	60	313741601	1267652262	7.0611	9.2351	0.9998	0.0023
4	99	260258241	1145078241	5.9506	8.4784	1.0002	0.0023
5	150	305560766	968166998	6.7962	6.9633	0.9988	0.0023
6	30	124542055	419067948	6.6987	7.2878	0.9986	0.0023
7	90	343703768	1039755550	7.8225	7.6513	0.9986	0.0023
8	1	281233879	1227303987	6.3320	8.9266	0.9978	0.0023
9	240	366815490	1148159992	8.2939	8.4038	0.9998	0.0023
10	180	279509932	1197032197	6.3536	8.8108	1.0001	0.0023

The sample-specific purities are displayed as functions of 1H -NMR analysis and bottle fill orders in Fig. 16. Analysis order may have a small influence on the purity estimates; there is no apparent influence from the source of the sample (Jars 1 and 2) or the bottle fill order.

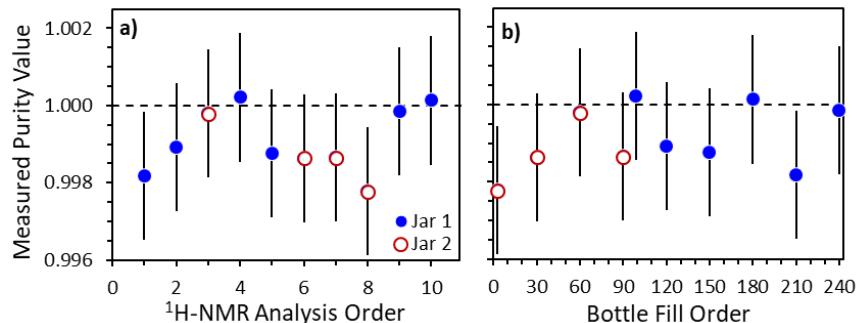


Fig. 16. Sample-Specific Purities as Functions of $^1\text{H-NMR}$ Analysis and Bottle Fill Orders.

Solid circles denote samples derived from the bulk material in Jar 1; open circles denote samples derived from Jar 2. Error bars represent standard uncertainties. The dashed horizontal lines represent the limiting purity mass fraction of 1 g/g.

Panel a) Sample-specific purity estimates as a function of $^1\text{H-NMR}$ analysis order, 1 to 10.

Panel b) Sample-specific purity estimates as a function of bottle fill order, 1 to 240.

4.3.2. $^1\text{H-qNMR}_S$ Purity

Several of the sample-specific purity estimates exceed the limiting purity mass fraction of 1 g/g. The w_p for the entire SRM 1595a production was calculated using a Bayesian procedure modeled on “observation equations” in accordance with Eq. (1), executed via Markov Chain Monte Carlo (MCMC) methods using OpenBUGS software [9]. The model used for this assessment is congruous with approaches described in [6,10], whereby the result is constrained to lie along the interval (0 to 1) g/g. Sampled units were grouped in two blocks according to the jar of bulk material from which they were filled. Samples from the two jars were treated as statistical blocks in the model because the two containers were delivered by the distributor at different times and exposed to slightly different environments for at least several weeks between deliveries. This approach was intended to allow possible heterogeneity arising from inconsistencies in material composition to be easily discerned and evaluated.

The purity estimates for the two jars were not related using a hierarchical model, as is typically done according to the method described in [6]. Rather, they were combined using a linear pooling procedure. A logistic (logit) transformation was applied to the estimate of w_p corresponding to each jar. This transformation was necessary for the model to successfully sample the posterior distribution because the result lies along a narrow value interval that is near the 1 g/g limit. The statistical model is hierarchical in terms of the logits of w_p for each jar. These logits were then blended using a linear pool procedure.

Calculation of uncertainty in this fashion is a hybrid “top-down”, “bottom-up” approach that includes the variation associated with the terms of the Eq. (1) measurement function, analysis of the 10 units sampled from across the production lot, and the between-jar variation.

The following Sections document the OpenBUGS code and measurement data used to estimate the tripalmitin purity for SRM 1595a Tripalmitin.

4.3.2.1. OpenBUGS Code

```
# Inputs
# Areal      2x6 matrix of mean  $A_i/N_i$ 
# Arealu     2x6 matrix of  $u(A_i/N_i)$ 
# AreaP      2x6 matrix of mean  $A_P/N_P$ 
# AreaPu     2x6 matrix of  $u(A_P/N_P)$ 
# avgmC      2x6 matrix of  $m_c$ 
# avgml      2x6 matrix of  $m_i$ 
# mImCu      scalar  $u(m_i)$  and  $u(m_c)$ 
# N          vector number of replicates per jar
#
# Outputs
# P          vector mass fraction purity per jar
# PLP        Scalar linear pool of jar purities
#
# Working variables
# Arealp     2x6 matrix of  $p(A_i/N_i)$ 
# AreaPp     2x6 matrix of  $p(A_P/N_P)$ 
# avgl       2x6 matrix of mean Areal distribution ( $t$ , 2 degrees of freedom)
# avgP       2x6 matrix of mean AreaP distribution (normal)
# i          scalar index over jars
# j          scalar index over replicates
# korig      2x6 matrix distribution width for avgl and avgP
# k.cut      2x6 matrix non-inferential version of korig
# mC         2x6 matrix normal prior for mC
# ml         2x6 matrix normal prior for ml
# mImCp      scalar precision form of mImCu (1/variance)
# mwI        scalar distribution  $M_i$  (molecular weight of tecazene)
# mwP        scalar distribution  $M_P$  (molecular weight of tripalmitin)
# Plogit     vector log-space estimate of P
# PlogitLP   linear pool: log-space estimate of PLP
# R          vector, linear pool: Dirichlet prior for T
# S          vector, linear pool: shape parameters for R
# T          scalar, linear pool: multinomial categorical distribution on the PlogitLP
# TCZ       scalar normal prior for the tecazene internal standard
#
# Model
{TCZ~dnorm(0.9979, 1234568); mImCp<-1/(mImCu*mImCu)
#
# calculate purity of samples from Jar i, i = 1 to 2
for(i in 1:2){
  mwI[i]~dnorm(260.883,10000); mwP[i]~dnorm(807.319, 1111)
  Plogit[i]~dnorm(5.0,0.2); P[i]<-ilogit(Plogit[i])
  for(j in 1:N[i]){
    korig[i,j]~dunif(0,0.01); k.cut[i,j]<-cut(korig[i,j])
    ml[i,j]~dnorm(avgml[i,j],mImCp); avgl[i,j]<-TCZ*ml[i,j]/(mwI[i]*korig[i,j])
    Arealp[i,j]<-1/(Arealu[i,j]*Arealu[i,j]); Areal[i,j]~dt(avgl[i,j],Arealp[i,j],2)
    mC[i,j]~dnorm(avgmC[i,j],mImCp); avgP[i,j]<-P[i]*mC[i,j]/(mwP[i]*k.cut[i,j])
    AreaPp[i,j]<-1/(AreaPu[i,j]*AreaPu[i,j]); AreaP[i,j]~dnorm(avgP[i,j],AreaPp[i,j])}
#
# Combine estimates for the two jars using linear pool procedure
for(i in 1:2){S[i]<-1}; R[1:2]~ddirich(S[]); T~dcat(R[]); PlogitLP<-Plogit[T]; PLP<-ilogit(PlogitLP) }
```

4.3.2.2. OpenBUGS Data

```
list(mImCu=0.0000005,N=c(3,3,3,4,3,3,3),  
avgmI=structure(.Data=c(0.008478,0.010418,0.006963,0.008811,0.010397,0.008404,  
0.008927,0.007288,0.009235,0.007651,NA,NA),.Dim=c(2,6)),  
avgmC=structure(.Data=c(0.005951,0.006404,0.006796,0.006354,0.005889,0.008294,  
0.006332,0.006699,0.007061,0.007823,NA,NA),.Dim=c(2,6)),  
Areal=structure(.Data=c(1.145078,1.422374,0.968167,1.197032,1.479459,1.14816,  
1.227304,0.419068,1.267652,1.039756,NA,NA),.Dim=c(2,6)),  
Arealu=structure(.Data=c(0.000573,0.000711,0.000484,0.000599,0.00074,0.000574,  
0.000614,0.00021,0.000634,0.00052,NA,NA),.Dim=c(2,6)),  
AreaP=structure(.Data=c(0.260258,0.282777,0.305561,0.27951,0.270843,0.366815,  
0.281234,0.124542,0.313742,0.343704,NA,NA),.Dim=c(2,6)),  
AreaPu=structure(.Data=c(0.00039,0.000424,0.000458,0.000419,0.000406,0.00055,  
0.000422,0.000187,0.000471,0.000516,NA,NA),.Dim=c(2,6)))
```

4.3.2.3. OpenBUGS Results

Intrinsic to the MCMC approach, the outputs from the open bugs code are posterior probability distributions which characterize the state of knowledge of the parameters of interest. The posterior distribution was sampled a total of 300,000 times. Only the later 200,000 samples, thinned by a factor of 10, were used to determine the summary statistics of the result.

There is no chemically meaningful between-Jar heterogeneity. The posterior distributions for the results derived from each jar of bulk material are summarized in Fig. 17 in the form of boxplots. The greater precision of values for Jar 1 could be attributable to the greater number of samples, and thus observable data, prepared from this jar (six analyzed units) than from Jar 2 (four analyzed units).

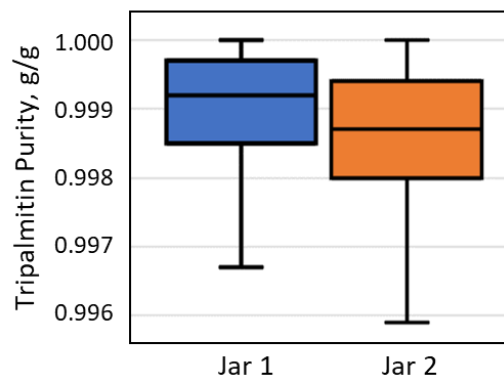


Fig. 17. Comparison of Purity Distributions for Units Derived from Jar 1 and Jar 2 Materials.

The upper and lower boundaries of the boxes represent the upper and lower quartiles of the sampled values. The center lines note the respective median sample values. The whiskers span the range of sample values.

The distribution for the estimate of SRM 1595a Tripalmitin purity is shown in Fig. 18. This distribution has a median value of 0.9990 g/g, standard uncertainty of 0.0009 g/g, and shortest 95% coverage interval along the value range [0.9968, 1.000] g/g. The distribution is highly skewed, with the longer tail extending along values less than the median. This asymmetry is largely due to the result lying so near the natural limit of the measurand, 1 g/g.

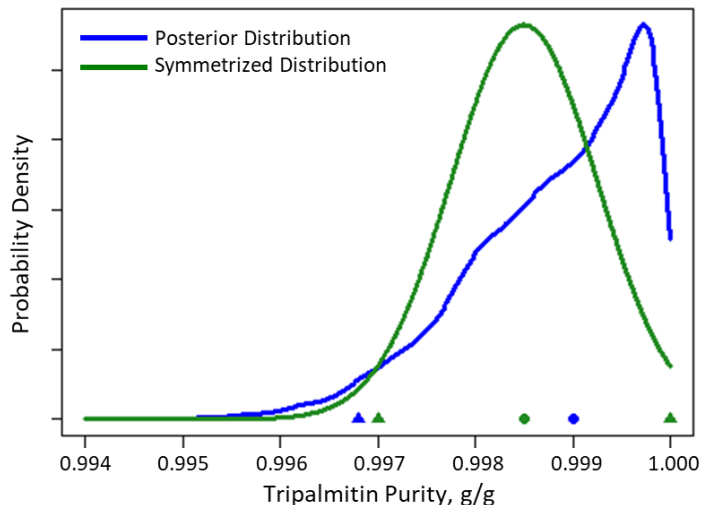


Fig. 18. SRM 1595a Purity Distributions.

The irregular blue curve represents the posterior distribution for the tripalmitin purity of SRM 1595a estimated using the OpenBUGS MCMC analysis. The smooth green line represents a symmetric Gaussian distribution that can be considered a fit-for-purpose approximation to the posterior in some applications. The color-coded circles along the horizontal axis denote the medians of the distributions; the triangles mark the shortest 95% coverage intervals.

It is recognized that the uncertainties denoting symmetric value intervals are often more convenient and accessible for many SRM users. Although not the preferred result delivered by the SRM 1595a, users may find it practical and adequate to treat the purity result as a symmetric (Gaussian) distribution when propagating the uncertainty of the certified value. For this purpose, the purity can be treated as (0.9985 ± 0.0015) g/g, where the number after the \pm symbol denotes uncertainty at approximately the 95 % level of confidence. The placement of the Gaussian distribution mean is reasonably consistent with the median of the posterior distribution (0.9990 g/g) and the symmetrized result covers nearly the entire 95 % coverage interval of the posterior. The difference between the lower 95 % coverage interval boundaries of the two distributions (0.02 %) is not chemically significant.

Whenever feasible, a more faithful representation of the asymmetric purity value interval [0.9968, 1.0000] g/g should be used with SRM 1595a. Parameterized as a beta distribution, the uncertainty can be propagated using tools such as the NIST Uncertainty Machine [11,12] or other programs for executing Monte Carlo Methods.

4.3.2.4. A Beta Distribution Approximation to the Posterior Distribution

Of the 10 000 MCMC data used to define the full posterior distribution, 3.4 % round to a value of 1 when reported to four significant figures. The exact value of 1 constitutes an event that has probability 0 under the beta distribution model [13]. Maximum likelihood estimation of the beta parameters cannot be accomplished in the presence of these 1s. To enable approximating the full distribution with a beta model using data expressed at this level of precision, values of 1 were replaced with random draws from a uniform distribution concentrated on the interval whose endpoints are the largest value in the sample that is smaller than 1, and 1. The kernel density estimate based on the results of this “accommodation” is depicted (thin blue curve) in Fig. 19.

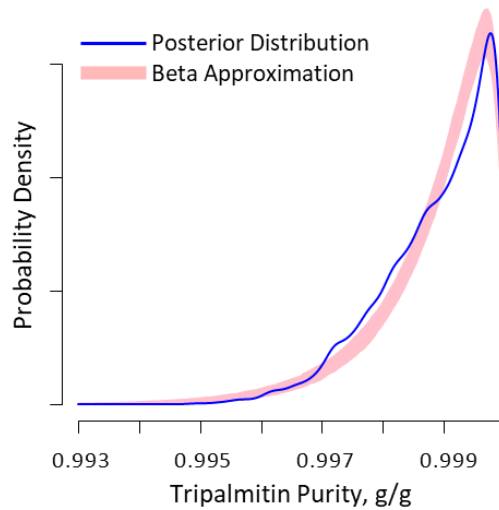


Fig. 19. Beta Distribution Approximation to the MCMC Posterior Distribution.

The irregular blue curve represents the limiting-value accommodation of posterior distribution for the tripalmitin purity of SRM 1595a estimated using the OpenBUGS MCMC analysis. The pink band is a 95% confidence envelope for the sampled beta distributions.

The corresponding maximum likelihood estimates of the beta parameters (as defined in [13]) and the large-sample approximation of their covariance matrix, are listed in Table 11. Both the estimates and their covariance matrix are relevant because, with great generality, the maximum likelihood estimates have a joint distribution that is approximately Gaussian [14]. In the present case, where there are two parameters, such joint distribution is bivariate. The covariance matrix elements are a by-product of the nonlinear optimization procedure that yields $\hat{\alpha}$ and $\hat{\beta}$.

Table 11. Maximum Likelihood Beta Parameters and Their Covariance Matrix.

Parameter	Value	Covariance Matrix	
$\hat{\alpha}$	1105.45	295.086	0.219153
$\hat{\beta}$	1.23458	0.219153	0.000244913

The results above can be used in two different ways to propagate the uncertainty that surrounds the purity and that is captured, approximately, by the beta distribution characterized in Table 11. One (S) is simple and very easy to use; the other (R) is more refined and propagates the uncertainty more accurately than (S). Both (S) and (R) involve drawing a value from a beta distribution, and then using it in some exercise of uncertainty propagation that uses a Monte Carlo method such as the NIST Uncertainty Machine [11]. In general, (R) is expected to yield larger (and probably more realistic) uncertainty evaluations for the end result than (S).

(S) Draw a value w_P of the purity from a beta distribution whose parameters have the values listed in Table 11.

(R) First, draw a pair (a, b) from a bivariate Gaussian distribution with mean $(\hat{\alpha}, \hat{\beta})$ as listed in Table 11, and with the covariance matrix specified in the same table, discarding any pair where either $a \leq 0$ or $b \leq 0$.

Second, draw a value w_P of the purity from a beta distribution with parameters a and b .

5. Water

The mass fractions of water in SRM 1595a was evaluated to ensure that it is compatible with the ^1H -qNMR_{IS} purity estimate. Water content was evaluated using volumetric Karl Fischer (KF) titration and thermogravimetric analysis (TGA).

5.1. Materials

The ten units of SRM 1595a used in the ^1H -NMR analysis described in Section 4. KF titration was used for the moisture analysis of three randomly selected units. All ten units were used for thermogravimetric analysis.

The reagents used in the KF system were Hydranal composite 2 (Fluka, lot SZBD3390V), methanol (Fisher, lot 161607), and chloroform (Fluka, lot I2620) (Fluka, lot SZBD2980V). Additional reagents used were one bottle of anhydrous 1-octanol obtained from Sigma-Aldrich (lot # SHBF8161V) and one bottle of LC-MS ultra chromosolve grade water obtained from Sigma-Aldrich (lot # BCBQ8032V). All reagents were reagent grade or higher unless noted otherwise.

SRM 917d D-Glucose (Dextrose) [15] and SRM 88b Dolomitic Limestone [16] were used as TGA controls.

5.2. Karl Fischer Titration

The water analysis was made on a volumetric KF system with Hydranal composite 2 as the KF reagent. The working solvent for the titration is a 1:1 (volume fraction) mixture of methanol and chloroform. Approximately 80 mL of the working solvent was added to the KF vessel. The entire apparatus is enclosed in a glove bag and is purged with dry nitrogen to minimize water uptake when the solid samples are added to the KF cell. The KF system was run overnight to fully equilibrate.

On the day of the test measurements, the titer (volume of solution delivered per mg of water consumed) of the Hydranal composite 2 solution was determined from several injections of an in-house standard of water saturated 1-octanol (WSO). The WSO was prepared in 2010 and stored on the benchtop at 22 °C, where the organic phase is used for the calibration. The WSO solution is periodically checked against gravimetrically prepared water in octanol solutions, and against SRM 2890 Water Saturated 1-Octanol [17] to confirm traceability [18]. The last full check was performed in December 2015. A more recent test performed during the characterization of SRM 916b Bilirubin [19] verified that the material is still fit for purpose. A minimum of three calibration measurements using 40 mg (nominal) of WSO were made by injecting the WSO into the KF titration vessel through a silicone septum via a gas-tight syringe. Samples of the WSO were weighed out on an analytical balance having 0.01 mg readability (Sartorius MC 210 S balance). The amount of WSO injected into the KF cell was determined by weighing the injection syringe before and after the injection on the analytical balance.

Following the calibration analyses, samples having nominal masses of 250 mg of SRM 1595a Tripalmitin were analyzed using the KF system. The samples were introduced into the system by

briefly opening the fill port and adding them via a glass weigh boat. The sample quantity introduced into the KF cell was determined to be the difference in mass between the weigh boat with and without the sample of SRM 1595a Tripalmitin.

All titrations were run for a set length of 40 minutes rather than a duration determined by the electrochemical potential of the cell alone. The drift of the instrument was calculated at the conclusion of every run over three successive 10-minute intervals to check for consistency in the baseline and to calculate the adjusted KF signal due to system drift.

After the analysis of every second sample, a blank titration was performed by opening the fill port and mimicking introduction of the sample using the weigh boat. On average, the blank correction for the KF analysis is (24 ± 5) μL of Hydranal composite 2 or (22 ± 4) μg of water.

The value for mass fraction of water in the sample, $w_{\text{H}_2\text{O}}$, is calculated:

$$w_{\text{H}_2\text{O}} = 10 \left(\frac{V_a - V_b - t \times R_d}{m} \right) F \quad (7)$$

where: V_a volume of titrant consumed by the tripalmitin,
 V_b volume of titrant consumed titrating a blank,
 t titration time,
 R_d drift rate,
 m mass of Tripalmitin, and
 F calibration factor determined by titrating WSO samples of known water content.

Table 12 reports the results for the three bottles of the of SRM 1595a Tripalmitin that were analyzed by KF titration. Results from these units were above the 41 μg H_2O limit of detection for the KF implementation but below its 82 μg H_2O limit of quantification (LOQ). Because of the low solubility of tripalmitin in the reagent, increasing the sample size to obtain a total mass of measurable water that is above the LOQ was not feasible. The large variability in the sample replicates precluded the use of this method as the primary water analysis technique.

Table 12. Karl Fischer Water Measurement Summary.

Unit	Replicate	Mass, g	Water, $\mu\text{g/g}$	
		m	$w_{\text{H}_2\text{O}}$	$u(w_{\text{H}_2\text{O}})^{\text{a}}$
180	1	0.22927	54	24
180	2	0.23964	103	23
99	1	0.24532	50	23
99	2	0.22796	225	25
1	1	0.26828	131	20
1	2	0.22066	50	22
		n :	6	
		Mean:	102	
		Standard Deviation:	69	23
		$u(\text{Mean})^{\text{c}}$:	30	
		$U(\text{Mean})^{\text{d}}$:	76	

Pooled $u(w_{\text{H}_2\text{O}})^{\text{b}}$

- a) Single-measurement uncertainty from the estimated uncertainties of the measurement equation parameters.
- b) Characteristic single-measurement uncertainty.
- c) Standard uncertainty of the mean, combining the standard deviation and the pooled $u(w_{\text{H}_2\text{O}})$ in quadrature, scaled by \sqrt{n} .
- d) Approximate 95 % level of confidence expanded uncertainty, estimated as the Student's t critical value for the 95th percentile with five degrees of freedom, 2.57, times the standard uncertainty.

5.3. Thermogravimetric Analysis

Ten units of SRM 1595a were evaluated for water by thermogravimetric analysis (TGA) using a Mettler Toledo Thermal Analysis System TGA2 analyzer. The procedure for loss of mass on heating with the TGA2 is in alignment with other published methods for thermogravimetric analysis (ASTM E2402-19) [20] and technical procedures for similar instrumentation.

Two test portions were removed from each bottle received and put into 600 μL alumina crucibles for analysis. The 10 units of SRM 1595a Tripalmitin were split into two runs of five bottles each. There was also an additional run of the control sample and a duplicate sample of one bottle of SRM 1595a using the same run conditions. Each crucible containing a test portion (nominally 150 mg for SRM 1595a and 250 mg for SRM 917d control) was transferred to the TGA to record an initial mass, m_0 . The samples were run in a random order to help mitigate any run order bias. The method used a simple ramp from 30 $^{\circ}\text{C}$ to 160 $^{\circ}\text{C}$ at a rate of 10 $^{\circ}\text{C}/\text{min}$. The mass of each sample was monitored by the TGA and was recorded approximately at a rate of 2 hertz.

After the sample analysis runs were complete, the data was analyzed using the Mettler STAR[®] software. Mass changes observed on the TGA thermogram were quantified by selecting points before and after the mass change (T_1 and T_2 , respectively), and taking the mass at each point (m_1 and m_2 , respectively). The midpoint of the mass change ($[T_2 - T_1]/2$) is the transition temperature and the change of mass, Δm , is calculated as $\Delta m = m_1 - m_2$. The mass fraction of water, $w_{\text{H}_2\text{O}}$, is calculated as:

$$w_{\text{H}_2\text{O}} = \left(\frac{m_1 - m_2}{m_0} \right) \text{g/g} . \quad (8)$$

The TGA thermograms showed a change in mass upon heating the tripalmitin samples with an observed midpoint near 105 °C; this is consistent with an expected midpoint for water loss. Results from the TGA for SRM 1595a Tripalmitin are given in Table 13. The average water mass fraction of SRM 1595a Tripalmitin as measured by TGA is 76.6 µg/kg with an approximate 95 % level of confidence expanded uncertainty of 17.3 µg/kg.

The measured water mass fraction for each unit is shown in Fig. 20. The units analyzed in Run 1 have slightly higher measured mass fractions of water than those in Run 2. This systematic between-Run bias is not uncommon for moisture values that are this low. There is no apparent bias between the materials derived from the two Jars, nor any trend attributable to the bottle fill order.

Table 13. Thermal Gravimetric Analysis Water Measurement Summary.

Run	Unit	Replicate 1			Replicate 2			Water, µg/g	
		m_o , mg	Δm , mg	w_{H_2O} , µg/g	m_o , mg	Δm , mg	w_{H_2O} , µg/g	w_{H_2O}	$u(w_{H_2O})^a$
1	3	150.3856	0.0119	79.0	151.4304	0.0126	83.1	81.1	17.0
1	30	159.2526	0.0145	90.7	166.7782	0.0116	69.3	80.0	26.5
1	99	157.8724	0.0121	76.5	153.0939	0.0152	99.1	87.8	29.5
1	150	158.7023	0.0116	73.3	158.5098	0.0118	74.1	90.2	27.1
1	240	152.1957	0.0120	78.8	159.0753	0.0139	87.5	83.1	18.7
2	60	167.3449	0.0111	66.5	165.3315	0.0112	67.8	67.2	18.1
2	90	161.8930	0.0104	64.4	164.4284	0.0106	64.4	64.4	15.7
2	120	159.7040	0.0108	67.4	164.8458	0.0121	73.4	73.7	23.7
2	180	157.6264	0.0131	82.9	152.8035	0.0149	97.6	70.4	18.5
2	210	167.2240	0.0096	57.4	160.6942	0.0126	78.5	68.0	24.9

n : 10

Mean: 76.6

Standard Deviation: 9.1 22.5 Pooled $u(w_{H_2O})^b$

$u(\text{Mean})^c$: 7.7

$U(\text{Mean})^d$: 17.3

- Replicate-measurement uncertainty from the estimated uncertainties of the measurement equation parameters combined in quadrature with the standard deviation of replication.
- Characteristic replicate-measurement uncertainty.
- Standard uncertainty of the mean, combining the standard deviation and the pooled $u(w_{H_2O})$ in quadrature, scaled by \sqrt{n} .
- Approximate 95 % level of confidence expanded uncertainty, estimated as the Student's t critical value for the 95th percentile with nine degrees of freedom, 2.26, times the standard uncertainty.

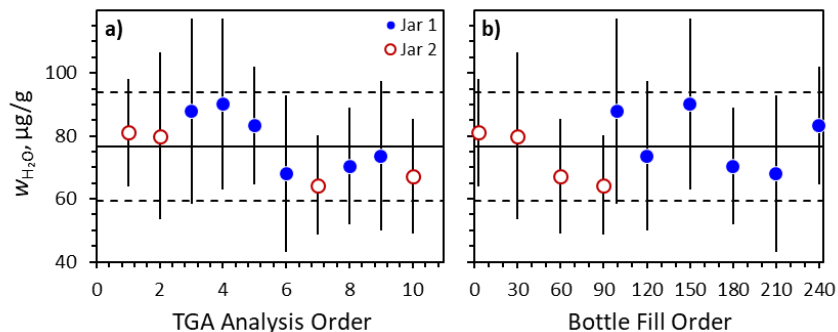


Fig. 20. Sample-Specific Water Content as Functions of TGA Analysis and Bottle Fill Orders.

Solid circles denote samples derived from the bulk material in Jar 1; open circles denote samples derived from Jar 2. Error bars represent standard uncertainties. The solid horizontal line represents the mean water mass fraction; the dashed horizontal lines bound the approximate 95 % confidence interval on the mean.

Panel a) Sample-specific water estimates as a function of TGA analysis order, 1 to 10, with analyses 1 to 5 in the first run, analyses 6 to 10 in the second.

Panel b) Sample-specific water estimates as a function of bottle fill order, 1 to 240.

While the measured (205 ± 105) $\mu\text{g/g}$ and certified (340 ± 110) $\mu\text{g/g}$ 95 % level of confidence intervals for the SRM 917d control overlap, chemically meaningful consistency among the two intervals is questionable. However, the TGA methods used for hydrophobic SRM 1595a tripalmitin may not be appropriate for the hydrophilic SRM 917d glucose in which water can be tightly bound.

Because of the differences in water binding properties between the SRM 917d and tripalmitin, a second control material was used. Most other potential control SRMs have a high affinity for water and/or a high vapor pressure, making it difficult to discern water mass loss from sublimation. Therefore, SRM 88b dolomitic limestone [16], whose change in mass upon heating is from loss of carbon dioxide rather than water, was used because the mass loss can be reliably measured using the same temperature ramp rate used for the tripalmitin measurements. The mass loss of SRM 88b measured by TGA, (0.46963 ± 0.00092) g/g, is in excellent agreement with the (non-certified) value for mass loss on ignition given on the certificate, 0.4698 g/g. Based on use of SRM 88b as a control, the measurements made on tripalmitin using TGA are considered valid.

5.4. Summary

The SRM 1595a units are homogenous with respect to water content, with no apparent differences attributable to the source of the material (Jar 1 and Jar 2) or bottle fill order (1 to 240).

The KF and TGA estimates for water mass fraction of (0.000102 ± 0.000076) g/g and (0.000077 ± 0.000017) g/g are compatible with the $^1\text{H-qNMR}_{\text{IS}}$ approximate 95 % level of confidence interval of [0.9968, 1.0000] g/g described in Section 4.

References

- [1] National Institute of standards and Technology (8 March 2022) Certificate of Analysis, Standard Reference Material 1595 Tripalmitin.
<https://tsapps.nist.gov/srmext/certificates/1595.pdf>.
- [2] Edwards S, Stribling S, Pyatt S, Kimberly M (2012) Reference measurement procedure for total glycerides by isotope dilution GC-MS. Clin Chem 58(4):768-776.
<https://doi.org/10.1373/clinchem.2011.177063>.
- [3] Milton MJT, Quinn TJ (2001) Primary Methods for the Measurement of Amount of Substance. Metrologia 38(4):289–296. <https://doi.org/10.1088/0026-1394/38/4/1>.
- [4] Jones GR, Jackson C (2016) The Joint Committee for Traceability in Laboratory Medicine (JCTLM) - its history and operation. Clin Chim Acta. 453:86-94.
<https://doi.org/10.1016/j.cca.2015.11.016>.
- [5] Panteghini M, Braga F, Camara JE, Delatour V, Van Uytvanghe K, Vesper HW, Zhang T for the JCTLM Task Force on Reference Measurement System Implementation (2021) Optimizing Available Tools for Achieving Result Standardization: Value Added by Joint Committee on Traceability in Laboratory Medicine (JCTLM). Clin Chem 67(12):1590–1605.
<https://doi.org/10.1093/clinchem/hvab178>.
- [6] Toman B, Nelson MA, Lippa KA (2016) Chemical Purity Using Quantitative ¹H Nuclear Magnetic Resonance: A Hierarchical Bayesian Approach for Traceable Calibrations. Metrologia 53(5):1193–1203. <https://doi.org/10.1088/0026-1394/53/5/1193>
- [7] Nelson MA, Waters JF, Toman B, Lang BE, Rück A, Breitruck K, Obkircher M, Windust A, Lippa KA (2018) A New Realization of SI for Organic Chemical Measurement: NIST PS1 Primary Standard for Quantitative NMR (Benzoic Acid). Anal Chem 90(17):10510-10517.
<https://doi.org/10.1021/acs.analchem.8b02575>
- [8] IUPAC Commission on Isotopic Abundances and Atomic Weights (CIAAW), molecular weight calculator. <https://ciaaw.shinyapps.io/calculator/>. Accessed August 31, 2022.
- [9] MRC Biostatistics Unit. The BUGS Project: OpenBUGS.
<https://www.mrc-bsu.cam.ac.uk/software/bugs/openbugs/>. Accessed 8/31/2022
- [10] Nelson M, Mulloor J, Lang B, Ishikawa M, Kondo Y, Toman, B (2022), Certification of Standard Reference Material®; 17g: Sucrose Optical Rotation, Special Publication (NIST SP), National Institute of Standards and Technology, Gaithersburg, MD,
<https://doi.org/10.6028/NIST.SP.260-217>.
- [11] Lafarge T, Newton D, Koepke, Possolo A (2023) NIST Uncertainty Machine, Version 1.6.1.
<https://uncertainty.nist.gov>.
- [12] Lafarge T, Possolo A (2020) NIST Uncertainty Machine – User’s Manual, Version 1.4.
<https://uncertainty.nist.gov/NISTUncertaintyMachine-UserManual.pdf>. See also: Lafarge T, Possolo A (2015) The NIST Uncertainty Machine, NCSLI Measure 10(3):20-27.
<https://doi.org/10.1080/19315775.2015.11721732>.
- [13] Beta Distribution. https://en.wikipedia.org/wiki/Beta_distribution. Accessed 12/1/2023.

- [14] Serfling RJ (1980). Approximation Theorems of Mathematical Statistics. Page 145. John Wiley & Sons, New York, NY. <https://doi.org/10.1002/9780470316481>.
- [15] National Institute of standards and Technology (18 January 2023) Certificate of Analysis, Standard Reference Material 917d D-Glucose (Dextrose). <https://tsapps.nist.gov/srmext/certificates/917d.pdf>.
- [16] National Institute of standards and Technology (20 May 1994) Certificate of Analysis, Standard Reference Material 88b Dolomitic Limestone. <https://tsapps.nist.gov/srmext/certificates/88b.pdf>.
- [17] National Institute of standards and Technology (9 June 2021) Certificate of Analysis, Standard Reference Material 2890 Water Saturated 1-Octanol. https://www-s.nist.gov/srmors/view_cert.cfm?srm=2890 .
- [18] Lang BE (2012) Solubility of Water in Octan-1-ol from (275 to 369) K, J Chem Eng Data 57(8):2221–2226. <https://doi.org/10.1021/je3001427>.
- [19] Nelson M, Brown Thomas J, Lang BE, Mulloor J, Sieber JR, Yu LL, Toman B, Lo S (2021) Certification of Standard Reference Material[®] 916b: Bilirubin. National Institute of Standards and Technology, Gaithersburg, MD, NIST Special Publication (NIST SP) 260-212. <https://doi.org/10.6028/NIST.SP.260-212>.
- [20] ASTM E2402-19, “Standard Test Method for Mass Loss, Residue, and Temperature Measurement Validation of Thermogravimetric Analyzers,” ASTM International, West Conshohocken, PA, United States (2019)

Appendix A. List of Abbreviations and Acronyms

^1H -qNMR _{IS}	quantitative proton nuclear magnetic resonance spectroscopy using an internal standard
$^1\text{H}\{^{13}\text{C}\}$ -NMR	one dimensional ^1H with ^{13}C decoupling NMR
ANOVA	Analyses of variance
CDC-NCEH-DLS	U.S. Centers for Disease Control and Prevention, National Center for Environmental Health, Division of Laboratory Services
ESI	electrospray ionization
FID	free induction decay
GSD	Global Spectral Deconvolution
HMBC	heteronuclear multi-bond coherence NMR
HRMS	high resolution mass spectrometry
HSQC	heteronuclear single quantum correlation NMR
IS	internal standard
KF	Karl Fischer
LOQ	limit of quantification
MCMC	Markov Chain Monte Carlo
NIST	National Institute of Standards and Technology
NMR	nuclear magnetic resonance spectroscopy
qNMR	quantitative NMR
SI	International System of Units (Système international d'unités)
SRM [®]	Standard Reference Material [®]
T1	spin lattice relaxation time
WSO	water saturated 1-octanol